The Effect of Soil Moisture on the Short-Term Climate and Hydrology Change—A Numerical Experiment

T.-C. YEH,[1] R. T. WETHERALD AND S. MANABE

Geophysical Fluid Dynamics Laboratory/NOAA, Princeton University, Princeton, NJ 08542

(Manuscript received 7 December 1982, in final form 21 December 1983)

ABSTRACT

This paper describes a series of numerical experiments simulating the effect of large-scale irrigation on short-term changes of hydrology and climate. This is done through the use of a simple general circulation model with a limited computational domain and idealized geography.

The soil at three latitude bands, namely 30°N–60°N, 0–30°N, and 15°S–15°N is initially saturated with moisture. The results from these experiments indicate that irrigation affects not only the distribution of evaporation but also that of large-scale precipitation. It is found that the anomalies of soil moisture created by irrigation of these respective latitude zones can persist for at least several months due to increased evaporation and precipitation. Furthermore, if the irrigated region is located under a rainbelt, precipitation in that rainbelt is enhanced. Conversely, if the irrigated region is not located under a rainbelt, much of the additional moisture is transported to a rainbelt outside this area. Thus the moist moisture anomaly for the 30°N–60°N case which is located under the middle latitude rainbelt tends to persist longer than the corresponding anomaly for the 0–30°N case.

Although both the 30°N–60°N and 15°S–15°N latitude regions occur under rainbelts, the soil moisture anomaly for the 15°S–15°N case does not persist as long as it does for the 30°N–60°N case. This is because in the 15°S–15°N case, a much greater fraction of the increased precipitation is lost from the hydrologic cycle due to runoff there as compared with the 30°N–60°N case.

The above changes of the hydrological processes also cause corresponding changes of the thermal state of the atmosphere such as a cooling of the surface due to increased evaporation. This results in changes of the mean zonal circulation through the thermal wind relationship. It is found that irrigation in the tropical region weakens the upward branch of the Hadley circulation in the vicinity of the tropical rainbelt.

1. Introduction

The influence of land surface processes on the weather or short-term climate change has been analyzed and discussed by Namias (1962, 1963). Also, more recent investigations have indicated that large changes of surface hydrologic conditions can lead to rather extensive variations of the hydrologic cycle. For example, Manabe (1975), Walker and Rowntree (1977), Kurbatkin *et al.* (1979), Shukla and Mintz (1982), Rind (1982) and Rowntree and Bolton (1983) investigated this problem using different versions of GCMs. In these studies, comparisons were made between numerical experiments in which relatively wet and very dry soil moisture conditions were used, respectively. The results from these various studies were, qualitatively, similar and indicated a considerable reduction of evaporation and precipitation over the anomaly areas for the dry cases as compared with the relatively wet cases. This reduction of evaporation and precipitation was found to be accompanied by an increase of surface temperature. This latter feature was caused by a reduction of latent heat flux by evaporation from the land surface. The results of these studies show that soil moisture can play an important role in determining regional climate and hydrology.

The purpose of the present investigation is fourfold. The first is to evaluate the persistence of soil moisture anomalies generated by very large-scale irrigation for three separate latitude zones. Since water vapor will, eventually, be transported out of the irrigated regions, it is of interest to determine the time scale of this removal. Secondly, it is of interest to evaluate the latitudinal dependence of the effect of the increased soil moisture on the short-term climate and hydrology. Since the prevailing atmospheric circulation is different from one latitude zone to another, it is worthwhile to study the various responses involved as a function of latitude. For example, the previous studies indicated that, although soil moisture was either systematically increased or decreased, the response of hydrology was far from uniform over the land areas considered in each investigation. It, therefore, seems desirable to attempt to understand this non-uniform response by designing a series of experiments to investigate how the persistence of a soil moisture anomaly depends

[1] On leave of absence from the Institute of Atmospheric Physics, Academia Sinica, Beijing, People's Republic of China.

upon latitude. A third purpose of this investigation is to evaluate the influence of irrigation upon the distribution of precipitation. And finally, changes of soil wetness can be expected to influence the thermal and dynamical state of the model atmosphere. Therefore a fourth purpose is to determine how the change in soil moisture conditions can alter the atmospheric circulation.

In the current investigation, a general circulation model with idealized geography will be used in order to easily identify the physical mechanisms responsible for the latitudinal changes of hydrology. This paper presents the results from a series of numerical experiments in which the soil moisture is artificially increased within three separate latitude zones.

2. The experimental plan

a. Brief description of the model

The model used for our study is the same as that used by Wetherald and Manabe (1981). It is similar to the model developed by Manabe and Stouffer (1980) except that it has a limited computational domain and idealized flat geography illustrated in Fig. 1. The model has three parts: 1) a general circulation model of the atmosphere, 2) a heat and water balance model over the continents and 3) a simple mixed-layer ocean.

In the atmospheric model the vertical component of vorticity, horizontal divergence, temperature, moisture and surface pressure are computed based upon the equations of motion, the thermodynamic equation and the continuity equations for moisture and mass. It is a spectral model truncated at wave number 15 in both the zonal and meridional directions. To ensure cyclic continuity of model variables between the two boundary meridians, only every third zonal wave component is retained in the model. In the vertical the model has nine unevenly-spaced finite difference levels. A semi-implicit method is used for time integration.

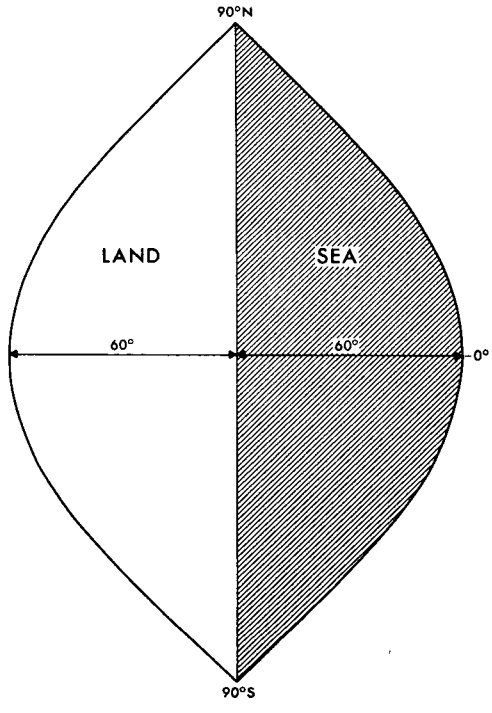

FIG. 1. Computational domain of the model.

The incoming solar radiation is prescribed at the top of the atmosphere as a function of latitude and season. The method for computation of solar radiation flux is similar to that described by Lacis and Hansen (1974). However, diurnal variation is not included in the model. For the computation of terrestrial radiation, the method developed by Rogers and Walshaw (1966) and modified by Stone and Manabe (1968) is used. In computing the fluxes of solar radiation and longwave radiation the mixing ratio of carbon dioxide is assumed constant everywhere; ozone is specified as a function of height, latitude and season; cloud cover is prescribed to be uniform zonally and invariant with respect to season; but water vapor distribution is determined by the prognostic equations.

Precipitation is predicted whenever supersaturation occurs. When the air temperature near the surface is below freezing, snowfall is forecast, otherwise rain is predicted. To incorporate moist convective processes a convective adjustment scheme is used (Manabe *et al.*, 1965).

In the heat and water balance model over the continent, the temperature of the continental surface is determined by the condition of local thermal equilibrium at a surface with no heat capacity. The soil albedo needed to determine the absorption of solar radiation at the ground is prescribed (see Manabe, 1969) rather than computed as a function of surface conditions such as soil wetness or type of vegetation. It is, however, replaced by a larger albedo in snow-covered areas. The change in snow depth is computed as the net contribution from snowfall, sublimation and snowmelt.

For computation of the water budget, the change of soil moisture is computed from the rates of rainfall, evaporation, snowmelt and runoff. The rate of evaporation from the soil is determined as a function of soil moisture and the potential evaporation, i.e., the hypothetical rate of evaporation from a completely wet soil surface. The maximum available soil moisture is assumed to be 15 cm for the sake of simplicity and to be consistent with previous studies. If the soil moisture content exceeds this value, runoff is predicted. More specifically, runoff is computed as the difference between the predicted soil moisture and 15 cm. The predicted soil moisture is then reset to 15 cm. For further details of the computation of the surface water budget, see Manabe (1969).

The ocean model is simply a mixed isothermal layer

with a uniform thickness of 68 m. In this simple model the horizontal ocean currents and the heat exchange between the mixed layer and the deeper layer of the ocean are neglected. The rate of temperature change in the ice-free region is computed from the net contribution of solar and terrestrial radiation fluxes and sensible and latent heat fluxes at the ocean surface. In the region with sea ice, the mixed layer temperature is fixed at −2°C, the freezing point of sea water, and the heat conduction through the ice is balanced by the latent heat of freezing (melting) at the bottom of the ice layer. This process, together with the melting at the ice surface, sublimation and snowfall determine the change in the ice thickness (Bryan, 1969). The albedo used in computing the net solar radiation at the oceanic surface is prescribed as a function of latitude, but over the areas covered by sea ice larger values are used.

Although the model described above has an idealized geography and prescribed cloudiness, it is very useful for identifying physical mechanisms which control climate and its response to changes of various parameters. The main purpose here is to illustrate physical processes influencing the short-term climate and hydrologic changes produced by irrigation rather than obtaining quantitative estimates of these effects for the real atmosphere. Despite the simplicity of the continental distribution, the model is still capable of generating a fairly realistic climate and hydrology. An example of this is shown in Fig. 2 which illustrates the latitudinal and seasonal variation of the zonally averaged precipitation rate over the model continent. This figure indicates that the model successfully reproduces the latitudinal excursions of the rainbelts in middle latitudes and tropics.

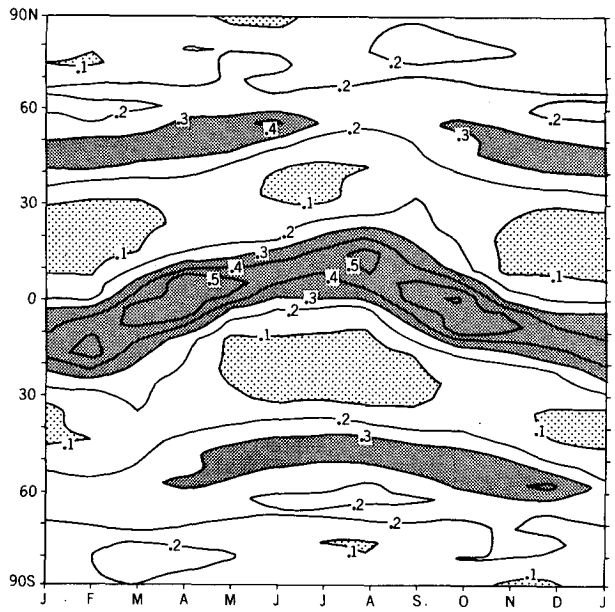

FIG. 2. The latitude-time variation of the zonal mean precipitation rate over the continent from the standard experiment. This figure is reproduced, in part, from a study by Manabe *et al.* (1981). Units: cm day^{-1}.

b. The experimental design

The sector model described above was integrated for a total of 19 years [see Wetherald and Manabe (1981) for the method of integration]. Climatic equilibrium was reached for all seasons after 13 years. The last four years of this entire integration were then averaged and served as the standard experiment for the above study as well as the present one.

Because of its capability in simulating the climate and hydrology, this model is convenient for pilot studies in exploring certain physical processes, especially those related to climate sensitivity to various external forcings. Comparisons are made between the standard experiment and the results of new perturbed experiments. There are three sets of new integrations corresponding to the three separate cases considered in this study. These are the 30°N–60°N, 0–30°N, and 15°S–15°N latitude zones, respectively. For the first set or the 30°N–60°N case, the soil is initially saturated on 1 July of each of the four separate years of the standard experiment. Each of the four runs is, then, integrated for a period of five months. The results of the four runs are averaged together and compared with the standard experiment. In the second and third sets, the latitude bands of 0–30°N and 15°S–15°N are, initially saturated with water on 1 January, respectively. The integrations, then, proceed in a similar manner as in the first set of experiments.

It should be pointed out that one of the purposes of the present paper is to study the latitudinal dependence of climatic and hydrologic response to an anomaly of soil moisture produced by a large scale irrigation. For this purpose, it would be more consistent to saturate the soil of the different latitude belts on the same date. However, in the standard experiment, the soil during the summer months is quite dry from subtropical latitudes poleward and wet in low latitudes, while in winter months, the opposite is true. In order to study the effect of supplying water to the soil, obviously a drier period should be chosen for study. Therefore, 1 July is chosen for 30°N–60°N case and 1 January is chosen for both 0–30°N and 15°S–15°N cases. A list of the three separate cases is given in Table 1.

TABLE 1. A list of the three separate experiments conducted in this study and their respective periods of integration.

Experiment number	Region of irrigation	Starting date	Ending date
1	30°N–60°N	1 July	30 Nov
2	0–30°N	1 Jan	31 May
3	15°S–15°N	1 Jan	31 May

The zonal mean value of water initially supplied to the soil as a function of latitude for the three cases is shown in Fig. 3. It may be seen that this amount varies considerably with the latitude for the 30°N–60°N belt, whereas it is approximately uniform with latitude for the other two cases. This is because the soil for the 30°N–60°N belt is quite wet in the northern portion during July. It may also be seen that the total amount of water added to the 30°N–60°N belt is considerably less than that added to the other two belts.

3. The enhancement of the hydrological processes

When water was added to the soil, evaporation from the surface became greater. This, in turn, increased the water vapor content of the model atmosphere. For the current study, the increase of atmospheric water vapor resulted in enhanced precipitation, thereby influencing the persistence of the soil moisture anomaly. This modification of the hydrological processes will be extensively discussed in the following section.

a. The response of soil moisture

In studying the response of soil moisture to irrigation, our main concerns are two-fold. One is to find out how long the anomaly in soil wetness can last. The second is to see whether or not the anomaly of the soil moisture is confined to the region of irrigation. Figs. 4a, 4b and 4c illustrate respectively the latitude–time distributions of differences of zonal mean soil moisture between the three perturbed experiments (i.e., the 30°N–60°N case, the 0–30°N case, and the 15°S–15°N case) and the standard experiment. In all three cases, this positive anomaly of soil moisture resulting from the irrigation persists at least two months. For further examination of these results, the normalized soil moisture anomaly, $\Delta W(t)_l/\Delta W(0)_l$, is plotted in Fig. 5 for each of the three experiments. Here, $(\ )_l$ denotes zonal average of ( ) over the continent and t is the time elapsed since the irrigation. In addition, the confidence interval of normalized soil moisture at the 90% level is indicated by a vertical bar. According to this figure, the positive anomaly persists about 5 months for the 30°N–60°N-case, and about 4 and 3 months for the cases of 0–30°N and 15°S–15°N, respectively.

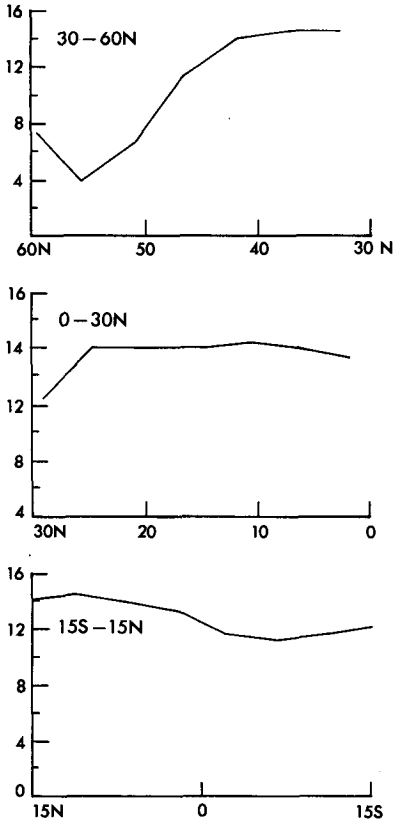

FIG. 3. Zonal mean moisture (cm) initially added into the soil for the three latitude belts considered in this study. For this and all subsequent figures, only the results over the land area are shown.

The second feature to be noted in Fig. 4 is that the increase of soil moisture is not limited to the latitude belt where water is added to the soil. Increased soil moisture is also observed outside this region. For example in the case of 0–30°N (Fig. 4b), there are two belts of increasing soil moisture, one to the north and the other to the south of the irrigated region. Soil moisture also increases on both sides of the irrigated region in the 30°N–60°N case although the southern belt of enhanced wetness is not so pronounced. In the 15°S–15°N case (Fig. 4c) one cannot identify these additional belts outside the influence region. However, it is of interest that in this case, the latitude–time distribution of zonal mean difference is not symmetric with respect to the center of the region of irrigation (i.e., the equator). The axis of maximum increase is clearly displaced to the Southern Hemisphere. The reasons for the two extra belts of increased soil moisture in Figs. 4a and 4b and the asymmetric bias of the axis of maximum increase are related to one another. For the time being we shall not discuss the reasons for these phenomena but will return to this subject in Section 3d.

To estimate the statistical significance of the main results of the present study, a Student's t test was performed on the difference distributions of the hydrologic quantities presented in this section. This statistical analysis is given in the Appendix.

Figs. A1 (a–c) of the Appendix show the Student's t analysis as performed on the latitude–time difference distribution of soil moisture for the 30°N–60°N, 0–30°N, and 15°S–15°N cases, respectively. According to Fig. A1, most of the features described above are statistically significant at the 90% (or higher) confidence level for all three cases. These features include the belts of enhanced wetness on both sides of the irrigated region in the 0–30°N case (see Fig. A1b). The statistical significance of the results is underscored by the fact

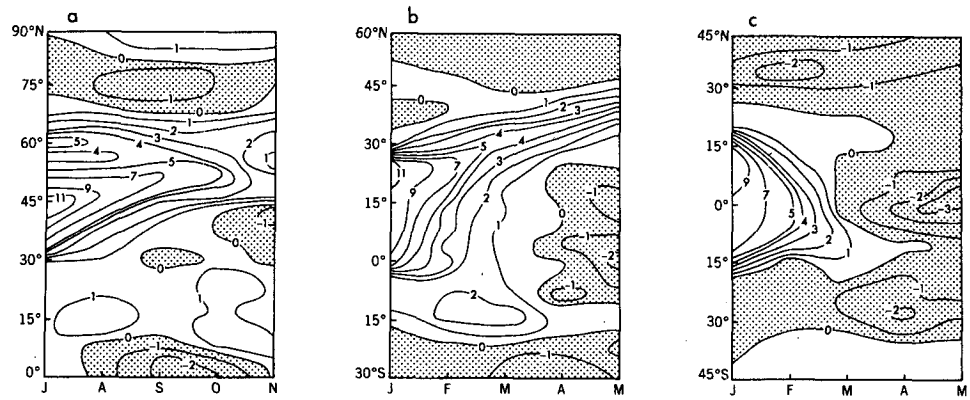

FIG. 4. The latitude–time distribution of the zonal mean difference of soil moisture (cm) between the perturbed and the normal experiment. (a) the 30°N–60°N case; (b) the 0–30°N case; (c) the 15°S–15°N case.

that, in each case, the soil moisture anomalies from all four runs exhibit these features.

b. *The enhancement of evaporation*

Figs. 6a–c show the latitude–time distributions of the differences of zonal mean rate of evaporation from the land between the three perturbed runs and the standard run. Comparing Figs. 6a, 6b and 6c with Figs. 4a, 4b and 4c, one notes that the distributions of the change in the rate of evaporation are very similar to the distributions of soil moisture change resulting from irrigation. For example, the period of enhanced evaporation is very similar to that of increased soil moisture in all three experiments. Furthermore, the evaporation rate increases not only in the latitude-belt of irrigation but also in areas outside the belt. The reason for such an increase will be discussed in Section 3d.

Figs. A2a, b and c of the appendix show the results from the Student's t analysis which is performed on the latitude–time difference of evaporation for the 30°N–60°N, 0–30°N and 15°S–15°N cases, respectively. According to this figure, the main features discussed in the preceding paragraph are statistically significant at the 90% (or higher) confidence level.

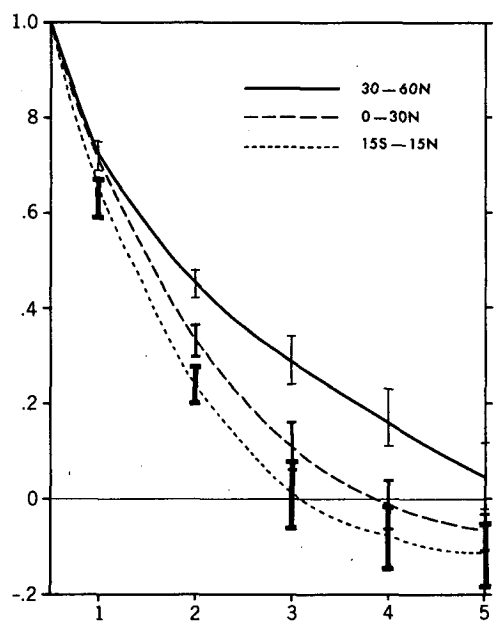

FIG. 5. Temporal variation of the normalized soil moisture anomaly obtained from the three separate cases. Values represent integrals taken over the entire latitude belts. The abscissa indicates months. The vertical line segments indicate the 90% confidence intervals resulting from a Student's t analysis at the 90% confidence level.

c. *The enhancement of precipitation*

It was stated in the beginning of this section that the large increase of evaporation from the ground resulted in an increase of water vapor content in the atmosphere, which in turn caused an enhancement of precipitation. Figs. 7a–c show the latitude–time distributions of the differences in zonal mean rate of precipitation between the three perturbed experiments and the standard experiment. One common feature in all the three figures is the increase of precipitation in the regions where the soil is instantaneously saturated with water. However, it is clear that the period of increased precipitation lasts the longest in the 30°N–60°N case and shortest in the 15°S–15°N case. The difference in the period of enhanced precipitation among the three cases is qualitatively similar to the difference in the persistence of the soil moisture anomaly or enhanced evaporation. The physical reason for this difference will be discussed in Section 3d.

In all three cases precipitation increased in the irrigated region but the latitude–time distribution of the difference in zonal mean precipitation rate is different for each separate case. In the 30°N–60°N case (Fig. 7a), the increase is at a maximum near the center of

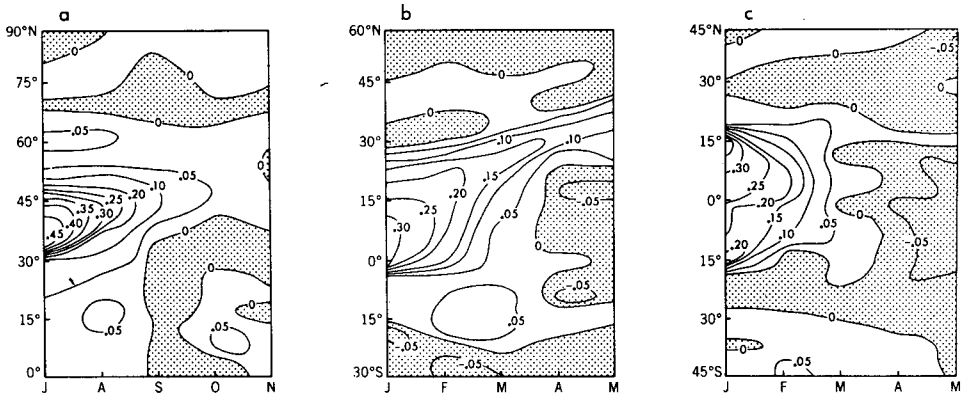

FIG. 6. The latitude–time distribution of the zonal mean difference of the rate of evaporation (cm day^{-1}) between the perturbed and the normal experiment. (a) the 30°N–60°N case; (b) the 0–30°N case; (c) the 15°S–15°N case.

the irrigated region and decreases both northward and southward. The corresponding distribution for the 15°S–15°N (Fig. 7c) is less symmetric. Its maximum is displaced to the Southern Hemisphere in January and shifts equatorward during February and March. For the 0–30°N case (Fig. 7b), there is no well-defined maximum of precipitation increase within the irrigated zone; instead, relatively small increases take place throughout the entire region.

Figures 7a and 7b share another common characteristic. Both show two belts of maximum increases, one to the south and the other to the north of the irrigated region. In the 30°N–60°N case the northern belt of maximum increase is in the latitude belt from 60–65°N and lasts for two months. The other belt is in the tropics and persists for a much longer period. It is also noted that the tropical belt shifts equatorward from July to November. In the 0–30°N case the northern belt of maximum increase is located near 40°N and the southern belt of maximum increase is situated at about 10°S. Both of these belts are outside the irrigated region.

Comparing Figs. 7a–c with the annual variation of the distribution of monthly mean precipitation of the standard run (Fig. 2), one notes that the increase of precipitation is much less in regions where it is normally dry, than in regions where rainbelts are located. This is especially pronounced in the 0–30°N case (Fig. 7b). In this case the increase of precipitation over the irrigated region is much less than the corresponding increase over the belts at both sides of the region. This is because the downward motion branch of the Hadley circulation is located at about 20°N. In the preceding analysis of the evaporation anomaly it was shown that the positive anomaly of evaporation is very high in this latitude belt. However, the enhancement of precipitation in this region is not very great because much of the additional evaporated moisture is exported to the nearby rainbelts by the divergent flow in the lower model troposphere. This topic will be discussed further in Section 3d.

Comparisons of Fig. 7 with Fig. 2 further show that the northern belts of maximum increase in precipitation in Fig. 7a (summer) and 7b (winter) are near

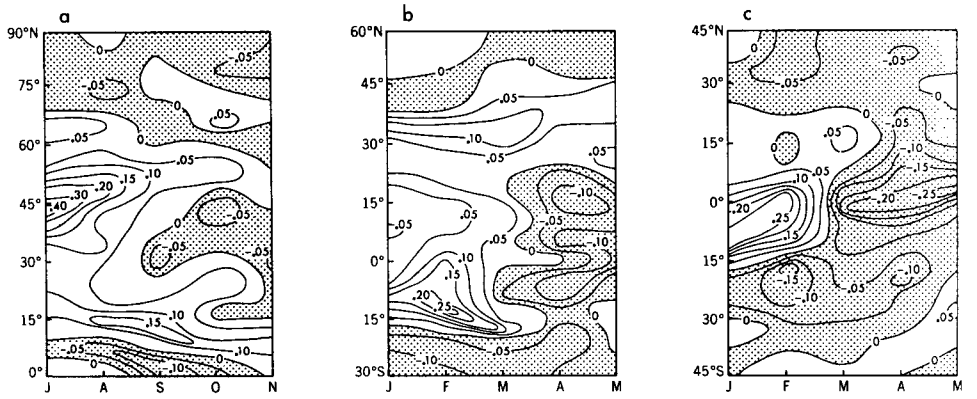

FIG. 7. The latitude–time distribution of the zonal mean difference of precipitation rate (cm day^{-1}) between the perturbed and the normal experiment. (a) the 30°N–60°N case; (b) the 0–30°N case; (c) the 15°S–15°N case.

the midlatitude rainbelts of summer and winter, respectively. The southern belts of maximum increase in precipitation in Figs. 7a and 7b are situated over the ITCZ rainbelt which is north of the equator and south of the equator, respectively. This indicates that a large-scale increase of soil moisture content can induce certain physical processes that enhance the activity of the ITCZ and midlatitude rainbelt even outside the region of the soil moisture increase. Although the physical reasons for these enhancements are not yet understood fully, it may be speculated as follows. The strengthening of evaporation due to irrigation will produce a sheet of moist and cold air near the ground (see Section 4). This sheet of moist and cold air spreads out of the region and supplies more moisture to the neighboring rainbelts. Thus the precipitation in these rainbelts is increased.

It is interesting to note, however, that for all three cases, precipitation actually decreased just to the south of the areas of maximum increase in the tropical rainbelts. Although this reduction may be related to changes of the upward motion in these regions (see Section 5b), the basic mechanism responsible for this characteristic is still under investigation.

The Student's t analysis as performed on the latitude–time difference distribution of precipitation rate for the 30°N–60°N, 0–30°N and 15°S–15°N cases is shown in Figs. A3a, b and c, respectively. In general, the statistical significance of the difference in precipitation rate is lower than those of the differences in soil moisture and evaporation rate due to the large temporal fluctuation of precipitation rate. However, most of the features of the difference in precipitation rate described above are statistically significant at the 90% (or higher) confidence level. This includes the increase of precipitation rate inside the irrigated regions for all three cases as well as the increase of precipitation rate outside the irrigated regions for both the 30°N–60°N and 0–30°N cases. Also significant is the decrease or reversal of the precipitation rate inside the irrigated region for the 15°S–15°N case for the last two to three months of integration. It may be seen that the increase of the precipitation rate inside the irrigated zone for the 0–30°N case is not as statistically significant as it is for the other two cases. This is consistent with the remarks made earlier in this section concerning the relatively small increase of precipitation rate for the 0–30°N case as compared with the other two cases.

d. The change of the surface water balance

The equation of change of water balance at the continental surface may be written as

$$\frac{\partial \Delta w}{\partial t} = \Delta r - \Delta e - \Delta f, \qquad (1)$$

where Δw is the difference of the soil moisture content between the perturbed experiment and the normal run and Δr, Δe and Δf are respectively the changes of rate of precipitation, rate of evaporation and rate of runoff from the standard run to the perturbed experiments. Figs. 8a–c show the temporal variation of monthly mean change of the water balance components for the 30°N–60°N, 0–30°N and 15°S–15°N cases, respectively. Comparing these three figures, one may see that the change of water balance due to large-scale irrigation is different from one case to another. For the 30°N–60°N experiment (Fig. 8a) the change of soil moisture for the first three months essentially results from the difference between the rate of precipitation and the rate of evaporation. The change of the rate of runoff is relatively small. In the first month (July), after saturating the soil with water, the rate of precipitation is increased by 0.18 cm day^{-1} from the standard to the controlled experiments and the rate of evaporation is increased by 0.29 cm day^{-1}. The corresponding increase of rate of runoff in this month is only 0.06 cm day^{-1}. These three hydrological processes together result in a decrease of the soil moisture content by 0.17 cm day^{-1} in the first month. In the second month (August) the changes in the rates of both precipitation and evaporation decrease. This results in an overall decrease of the rate of change of soil moisture from -0.17 cm day^{-1} in July to -0.08 cm day^{-1} in August. The rate of soil moisture change reduces with time after September.

For the 0–30°N case (Fig. 8b) the change of the rate of runoff between the perturbed and standard experiments is also small in the first two months (January and February) after the irrigation. In this case the increase of the rate of evaporation is much larger than the increase in the rate of precipitation. This causes the soil moisture content to decrease by 0.23 cm day^{-1} in January and 0.14 cm day^{-1} in February.

In the case of 15°S–15°N (Fig. 8c) the change of runoff rate plays an important role in regulating the change of soil moisture content for reasons to be given later. Its magnitude is roughly equal to the increase of the rate of precipitation in the first two months (January and February). This causes the rate of decrease of soil moisture content to be almost equal to the increase in evaporation.

It is further noted that in the 15°S–15°N (Fig. 8c) case there is sharp reversal of the processes of the main components of hydrology, namely precipitation, evaporation and runoff. In the first two months (January and February) all three components show a large increase from the normal to the perturbed experiment. During the third month (March) they all change sign and show a large decrease from the standard experiment to the perturbed one. Analysis of the four individual runs indicates that this reversal occurs in the third month of all simulations. Also, the statistical tests performed in the preceding sections show this reversal to be statistically significant (see Figs. A1c and A3c).

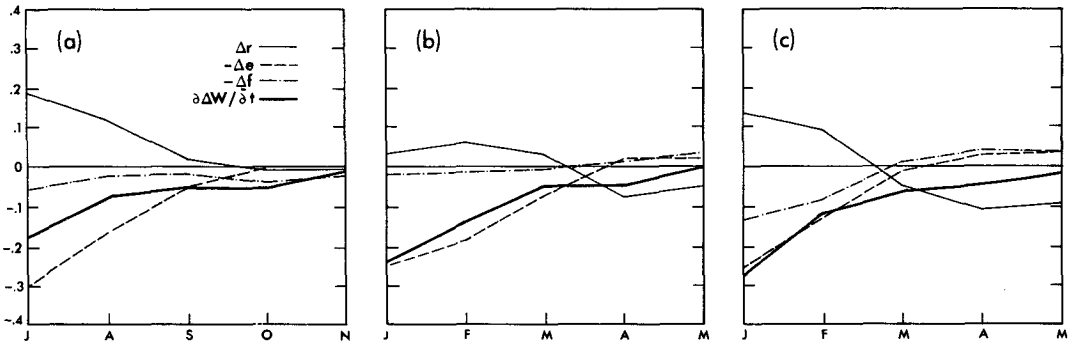

FIG. 8. The water balance components (cm day^{-1}) of the soil integrated over the entire latitude belt. Δr, the change of precipitation rate; Δe, the change of evaporation rate; Δf, the change of runoff rate; $\partial \Delta w/\partial t$, the rate of change of soil moisture. (a) the 30°N–60°N case; (b) the 0–30°N case; (c) the 15°S–15°N case.

The reason for the change of sign of precipitation difference for this particular case is not clear. It appears that the evaporation in the perturbed experiment increases to the point where it causes the soil to become much drier as compared with the standard experiment. The decrease in evaporation rate is accompanied by a decrease of the precipitation rate. This process is also shown in the 0–30°N case (Fig. 6b, 7b and 8b), but the time of the reversal appears later in the 0–30°N case than in the 15°S–15°N case. For the 0–30°N case the increase in precipitation over the tropical rainbelt induces subsidence over the water filled region. This may be partially responsible for the reversal. For the case of 30°N–60°N this reversal is not apparent, possibly because the time of integration is not long enough to allow it to appear.

In Section 3a, it was noted that the persistence of the soil moisture anomaly is longest in the 30°N–60°N case and shortest in the 15°S–15°N case. According to Fig. 3, the mean increase of soil moisture from the irrigation of the 30°N–60°N belt is less than the corresponding increase in either of the other belts. Therefore, it is clear that the difference in the amount of irrigation is not responsible for the longer response time for this region. In order to determine the reason for this difference among the three experiments, it is useful to reexamine Fig. 8. This figure clearly illustrates why the positive anomaly of soil moisture in a belt of irrigation persists longer in the 30°N–60°N experiment as compared with the 0–30°N experiment. In the 30°N–60°N experiment, the rate of rainfall increases substantially over the belt of irrigation, whereas it increases only slightly in the 0–30°N experiment. As discussed already, the middle latitude rainbelt is located in the 30°N–60°N belt. Therefore, an enhanced evaporation resulting from the irrigation in the 30°N–60°N belt increases the moisture supply to the rainbelt and enhances rainfall in the belt. Thus, moisture recycles in the belt of irrigation. (This is indicated by the compensation between Δr and $-\Delta e$ in Fig. 8a.) Accordingly the positive anomaly of soil moisture tends to persist over a long period of time. On the other hand, the winter irrigation in the 0–30°N belt increases the moisture supply to the middle latitude and tropical rainbelts which are located outside the zone of irrigation. In other words, a large fraction of the additional moisture is exported and does not remain in the belt of irrigation. Therefore, the positive anomaly of soil moisture does not last as long as the 30°N–60°N case. In short, the present results suggest that a soil moisture anomaly in a rainbelt tends to persist longer than a similar anomaly located outside the rainbelt because of a recycling of moisture (i.e., a return of moisture to the irrigated surface by precipitation that was previously evaporated from there).

To a close approximation, the moisture transported out of each irrigated zone is given by the integrated change of precipitation minus evaporation. This quantity is listed in Table 2 as $\Delta(P - E)$ where P is precipitation and E is evaporation. It may be seen from this table that $\Delta(P - E)$ has a larger negative value in the 0–30°N region than either of the other two latitude zones. This is consistent with the previous statements concerning the relatively large fraction of the supplied moisture transported out of the 0–30°N latitude belt as compared with the 30°N–60°N zone where more of the additional moisture is recycled within the irrigated region.

It is not obvious from the above discussion why the positive anomaly of soil moisture generated by irrigation in the 15°S–15°N belt does not persist longer

TABLE 2. Total integrated change of precipitation minus evaporation $\Delta(P - E)$ for the three latitude zones averaged over the period where values of ΔP were positive.

Latitude zone	$\Delta(P - E)$ (cm)
30°N–60°N	−5.7
0–30°N	−11.8
15°S–15°N	−5.2

than the anomaly in the 0–30°N experiment. Since the tropical rainbelt is located in the 15°S–15°N belt, the additional supply of moisture from the irrigation should enhance the precipitation in the belt by recycling water vapor and should prolong the duration of the soil moisture anomaly, as was the case in the 30°N–60°N experiment. The first expectation is substantiated by Fig. 8c which indicates a substantial increase in precipitation rate during a few months following the irrigation. However, Fig. 8c also indicates that the rate of runoff increases substantially during the same period in response to the irrigation. (Note that in Figs. 8a and 8b Δf is small as compared with Fig. 8c.) Because of a large standard deviation in the tropical rainfall rate, a substantial fraction of additional precipitation resulting from the irrigation increases the runoff rate rather than soil moisture, as seen in Fig. 8. Therefore, the soil moisture anomaly in the 15°N–15°S belt does not persist as long as the anomaly generated by the 30°N–60°N irrigation. In short, the tropical anomaly did not persist as long as the other anomalies because a large fraction of the additional moisture is lost through runoff despite the recycling of moisture by the atmospheric circulation.

One of the important factors which determine the duration of a soil moisture anomaly is the radiation energy absorbed by the earth's surface because it controls the rate of soil moisture depletion by evaporation. Thus the larger the absorbed radiative energy, the shorter the time required for a soil moisture anomaly to disappear. This implies that for a given season, the duration of a soil moisture adjustment in high latitudes is greater than a soil moisture adjustment in low latitudes. However it is important to note that, in the 30°N–60°N experiment, the summer insolation is imposed whereas in the other two experiments, the winter insolation is prescribed. Therefore, the insolations used for these three experiments are not very different from one another. This is the main reason why the changes in evaporation rate caused by irrigation are quite similar among the three experiments despite the large differences in the latitudes where irrigation is conducted. Since the insolations for the three separate cases are practically the same, this factor is not responsible for the difference in the persistence of the various soil moisture anomalies found in this study.

The effect of the soil moisture change upon the hydrologic processes may be best illustrated by Tables 3 and 4. Here for a particular latitude zone, ΔW_S represents the total integrated water supplied to the soil, ΔE is the total integrated increase of evaporation, ΔP is the total integrated increase of precipitation and ΔR is the total integrated increase of runoff due to the irrigation process (Table 3). From these quantities, the ratios $\Delta E/\Delta W_S$, $\Delta P/\Delta W_S$ and $\Delta R/\Delta W_S$ are computed (Table 4) which may be considered as a measure of efficiency of irrigation in inducing the change of precipitation rate. The larger the ratio $\Delta P/\Delta W_S$, the more benefit is gained from the irrigation. In the region where $\Delta P/\Delta W_S \sim \Delta E/\Delta W_S$ the benefit attains its optimum. In the region where $\Delta P/\Delta W_S \ll \Delta E/\Delta W_S$, the efficiency of irrigation becomes the least. From this viewpoint (see Table 4), the benefit of irrigation is largest in the 30°N–60°N, moderate in the 15°S–15°N zone and least in the 0–30°N zone. In the 15°S–15°N belt the efficiency of irrigation is not uniform. This may be seen by comparing Fig. 6c and Fig. 7c. Fig. 6c shows the maximum increase of evaporation near 15°N while Fig. 7c shows the maximum of precipitation near the equator or to the south of it. A similar feature is also evident for the belt of 30°N–60°N. For this belt the maximum increase of evaporation is centered near 35°N (see Fig. 6a) while the maximum increase of precipitation (Fig. 7a) is farther to the north. For the 0–30°N case, although the maximum increase of evaporation (Fig. 6b) is just north of the equator, the increase of precipitation (Fig. 7b) is small over the latitude belt of irrigation. All of the above discussion indicates that irrigation is least effective in the region of mean descending motion and is most effective in a rainbelt.

TABLE 3. Total integrated increases of the water balance components ΔE, ΔP, and ΔR due to an increase of soil moisture ΔW_S for the three latitude zones averaged over the period where the values of ΔP were positive. Units are centimeters.

Latitude zone	ΔW_S	ΔE	ΔP	ΔR
30°N–60°N	11.2	15.3	9.6	3.1
0–30°N	13.9	15.5	3.7	1.2
15°S–15°N	13.0	11.8	6.6	6.7

Another quantity of interest in this discussion is the integrated relative increase of precipitation $\Delta P/P$ which is given in the last column of Table 4 for all three cases. It may be seen that the variation of this quantity is very similar to that of $\Delta P/\Delta W_S$. Therefore, the relative increase of precipitation is largest for the 30°N–60°N case and smallest for the 0–30°N case which is consistent with the previous remarks concerning the efficiency of irrigation $\Delta P/\Delta W_S$ for these cases.

4. The change of thermal balance near the ground

One of the main effects of the hydrological change is the response of surface temperature (T_*). The dis-

TABLE 4. Ratios of the water balance increases given in Table 2 to the amount of soil moisture added for each latitude zone considered in this study.

Latitude zone	$\Delta E/\Delta W_S$	$\Delta P/\Delta W_S$	$\Delta R/\Delta W_S$	$\Delta P/P$
30°N–60°N	1.37	0.86	0.28	0.66
0–30°N	1.11	0.27	0.09	0.37
15°S–15°N	0.91	0.51	0.52	0.43

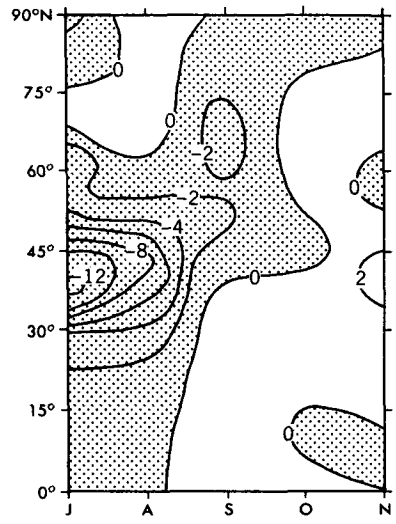

FIG. 9. The latitude–time distribution of the difference of zonal mean surface temperature (°C) of the soil for the 30°N–60°N case.

tribution of the latitude–time difference of zonal mean T_* between the perturbed and the standard experiments is very similar in all three cases. Fig. 9 shows the 30°N–60°N case as an example. In the region where the soil is saturated with water, T_* decreases everywhere from July to the end of September. The magnitude of the maximum reduction of T_* between perturbed and the standard experiments is 12°C. For the other two cases it is more than 10°C. Qualitatively similar results were previously obtained by other authors (e.g., Shukla and Mintz, 1982; Rind, 1982; Rowntree and Bolton, 1983).

In order to understand the reason for these reductions of surface temperature, the heat balance of the continental surface is analyzed. In the absence of snowmelt this may be written as

$$SW - LW - SH - LH = 0, \qquad (2)$$

where SW is the net solar radiation, LW is the net longwave radiation, SH is sensible heat flux, and LH is latent heat flux at the surface. Here, SW is defined as positive downward, whereas LW, SH and LH are considered positive upward. Because of the simplification made in the construction of the model, the contribution from the heat conduction through soil does not appear in this heat balance equation. The difference of these heat balance components between the perturbed and standard experiments may be derived from Eq. (2) as

$$\Delta SW - \Delta LW - \Delta SH - \Delta LH = 0, \qquad (3)$$

where Δ denotes the differences between the two experiments.

Figures 10a, 10b and 10c show the temporal variation of monthly mean difference of the surface heat balance for the 30°N–60°N, 0–30°N and 15°S–15°N cases, respectively. There are several features common to all three cases. These are: a) a small change of net solar radiation for the entire time period, b) a greater heat loss due to increased evaporation from the irrigated surface, and c) a decreased heat loss resulting from a reduction of both sensible heat and longwave radiation for the same time period. This analysis indicates that there is a large increase of ventilation of the model surface due to the relatively large increase of evaporation (see Section 3b) which manifests itself by a negative contribution to the surface heat balance (i.e., $-\Delta LH < 0$). This results in the reduction of surface temperature which, in turn, reduces the heat loss by both net longwave radiation and sensible heat changes (i.e., $-\Delta LW$ and $-\Delta SH > 0$). Since the heat gain through solar radiation hardly changes ($\Delta SW \approx 0$), the increase of ventilation through evaporation implies a smaller loss of heat by both net long wave radiation and sensible heat fluxes. These changes in the surface heat balance components are especially pronounced during the first two months of integration for all three cases.

Figure 10a shows that the four thermal components approach their normal values sometime in October, about four months after the irrigation in the 30°N–

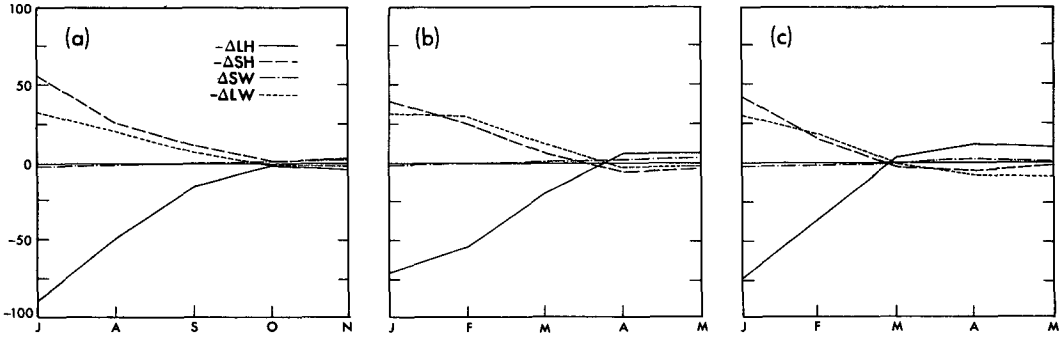

FIG. 10. The heat balance components W m^{-2} of the soil integrated over the entire latitude belt. ΔLH, the change of latent heat flux; ΔSH, the change of sensible heat flux; ΔSW, the change of solar radiation absorption; ΔLW, the change of longwave radiation emission.

60°N zone; while in Fig. 10b these four thermal components attain their normal values between March and April, about three and one half months after the irrigation in the 0–30°N zone. Fig. 10c shows that the four thermal processes reverse their sign between February and March less than three months after the irrigation in the 15°S–15°N zone. In other words, the response time of the heat balance anomaly is again longest for the 30°N–60°N case and shortest for the 15°S–15°N case. This is consistent with the analysis performed on the water balance components in Section 3d.

In all three cases, the very small differences in solar radiation between the standard and perturbed experiments are caused by the increase in the atmospheric moisture content. Because of this increase, the absorption of solar radiation in the atmosphere increases. Therefore, the solar energy received by the ground decreases slightly as Figs. 10a–c indicate.

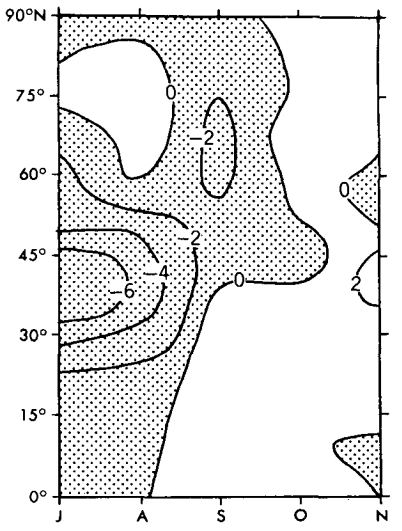

FIG. 11. The latitude–time distribution of the difference of zonal mean surface air temperature (°C) for the 30°N–60°N case.

5. The thermal response of the atmosphere and the change of circulation

In the previous section it was shown that large-scale irrigation can effectively reduce the sensible heat flux and long wave radiation from the earth's surface to the atmosphere. This will cool the atmosphere in the lower layer. But the precipitation enhanced by irrigation will release more latent heat and warm the atmosphere, probably in the middle troposphere. The resulting change of the thermal state of the atmosphere depends on the relative importance of these two processes and the relative position of the release or removal of heat. A modification of the thermal state of the atmosphere will invariably be accompanied by a corresponding change in the atmospheric circulation. The following section will deal with this topic.

a. The change of thermal state

Figure 11 shows the distribution of latitude–time zonal mean difference to T_9, the air temperature of the lowest level of the model, between the 30°N–60°N and the standard experiments. The pattern of this distribution is very similar to that of the difference of T_* shown in Fig. 9. The main difference is that the magnitude of the temperature change for T_9 is considerably less than that for T_*. For the 0–30°N and 15°S–15°N cases these distributions are very similar in nature to Fig. 11 and therefore are not shown.

The thermal influence of the large-scale irrigation as a function of height is illustrated in Figs. 12a–c. They show the latitude–height distribution of the zonal mean temperature difference between the perturbed and standard experiments in the second month after irrigation for the three cases. The three pictures show a common feature, a negative difference in the lower layer of the atmosphere above the irrigated zone and a positive difference higher up. This indicates that in the lower layer of the atmosphere the increase of latent heat flux by evaporation from the earth decreases the temperature, while at higher levels the increase of latent heat release from precipitation increases the temperature. Even two months after the large-scale irrigation, the maximum decrease of temperature is still nearly 6°C for both the 30°N–60°N case (Fig. 12a) and the 0–30°N case (Fig. 12b) and nearly 5°C for the 15°S–15°N case (Fig. 12c). The maximum increase in temperature in high levels reaches 1.8°C in the 30°–60°N belt, 2.4°C in the 0–30°N belt and nearly 3.0°C in the 15°S–15°N belt, respectively.

Another interesting feature in Fig. 12a and 12b is the asymmetric spreading of the cold anomaly in the lower layer of the atmosphere. In the case of 30°N–60°N the cold anomaly spreads southward all the way (see also Fig. 11) to the equator, while in the north it is limited to approximately 60°N. In the case of 0–30°N the cold anomaly (see −1°C isotherm) spreads far across the equator while in the north the cold anomaly is limited to approximately 33°N. This is due to the Hadley circulation which has a strong southward transport in the lower atmosphere from the subtropics (Northern Hemisphere) to south of the equator. It is this southward intrusion of cool, moist air that can supply moisture to the upward motion of the ITCZ and thus cause an increase of precipitation in the ITCZ.

For the case of 15°S–15°N the surface cold anomaly is fairly symmetric and limited primarily to the region of irrigation. This is because the irrigated region is situated under the area of ascending motion associated with the equatorial rain belt.

b. Change of vertical motion

It was shown previously that evaporation increased in response to an irrigation of the three zones consid-

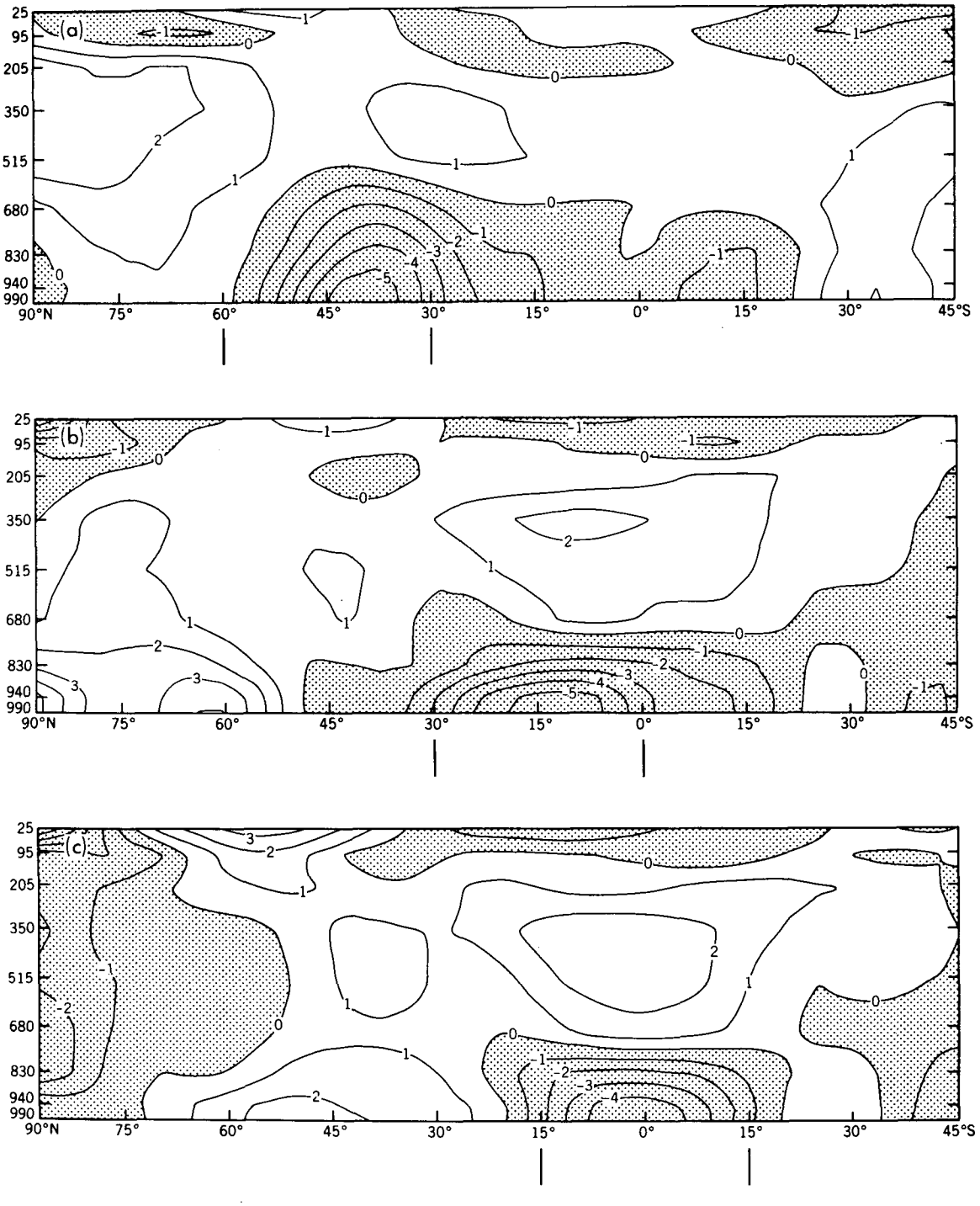

FIG. 12. The latitude–height distribution of the zonal mean difference of air temperature (°C) over land between the perturbed and normal experiment. (a) August of the 30°N–60°N case; (b) February of the 0–30°N case; (c) February of the 15°S–15°N case.

ered in this study. This, in turn, produced enhanced precipitation and lower surface air temperatures in these regions. Both of these tendencies affect the mean upward vertical motion in the tropical rainbelt. For example, the increase of precipitation enhances the release of latent heat and strengthens the upward velocity. On the other hand, the reduction of lower tropospheric temperature in the upward motion branch of the Hadley cell weakens the upward velocity there.

The net effect of these two opposing processes is

quite evident in the 15°S–15°N case where the irrigated zone is located under the tropical rainbelt. Figs. 13a, 13b show the latitude–height distributions of the February zonal mean ω (vertical p velocity) and the difference of ω for the 15°S–15°N case, respectively. In this figure, it may be seen that the upward velocity associated with the tropical rainbelt, centered at approximately 15°S, is generally weakened due to irrigation in the 15°S–15°N case. [Here, it should be noted that since the sign of ω is defined as negative (−) upward, a positive difference in the vicinity of the tropical rainbelt implies a weakening of upward velocity there.] A Student's t analysis performed upon the difference distribution of ω reveals this weakening of upward velocity in the vicinity of the tropical rainbelt to be statistically significant at the 90% confidence level (see positive shaded area of Fig. A4 of the appendix near 15°S). Evidently for this particular experiment, the increase of latent heat release in the upper model atmosphere was more than compensated by the decrease of surface temperature caused by the enhanced evaporation from the irrigated surface. Therefore, the upward velocity in the tropical rainbelt is weakened despite an increase of precipitation there. A similar tendency is observed for the 0–30°N case but the weakening of vertical velocity is not as statistically significant as it was for the 15°S–15°N case. As Fig. 12b and 13a indicate, the irrigated region for the 0–30°N case is located to the north of the rainbelt and its corresponding latitudinal area of surface temperature decrease extends under both the upward and downward branches of the Hadley circulation. Therefore, the overall effect of this temperature anomaly upon the upward branch of the Hadley circulation is more uncertain than it was for the 15°S–15°N case.

c. *The change of zonal circulation*

Since large-scale motion, especially the long-term mean, is quasi-geostrophic, there will be a change in the mean zonal circulation in response to the change of the zonal mean temperature. The latitude–height distribution of the zonal mean August difference of zonal wind between the 30°N–60°N and the standard experiments is given in Fig. 14. This figure clearly shows that to the south of 45°N there is a general increase of westerly wind speed and to the north of this latitude there is a general decrease of westerly wind. The maximum increase at about 34°N latitude and the maximum decrease at about 53°N latitude are of comparable magnitude. This change in zonal wind described here is consistent with the change in the zonal mean temperature field (Fig. 12a) which has a large latitudinal variation near 45°N in the lower atmosphere.

6. Summary

It is shown that large-scale instantaneous irrigation can initiate a feedback process enhancing various hy-

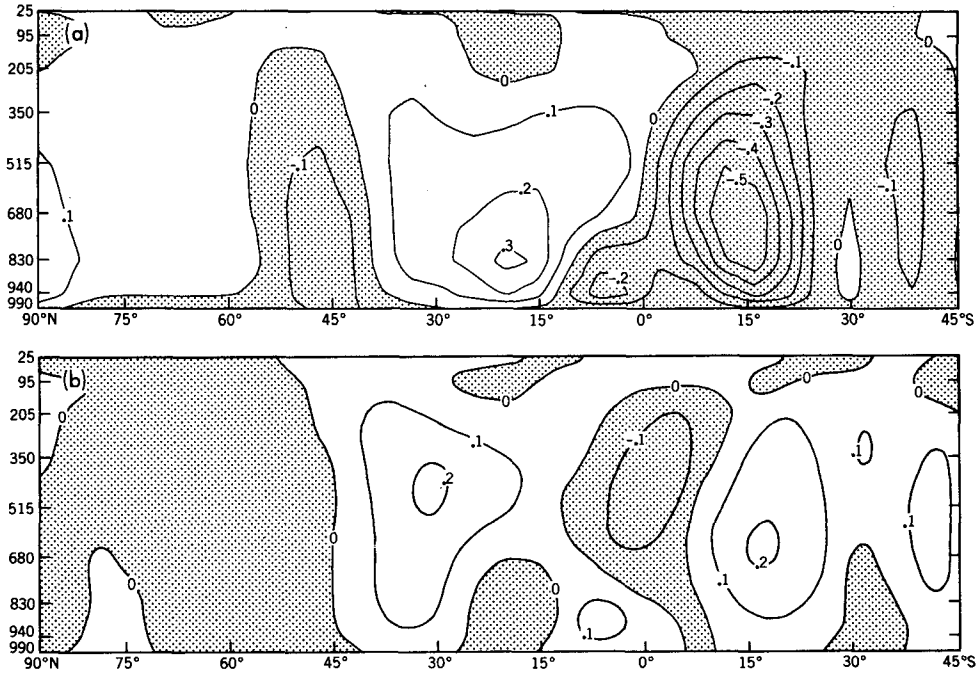

FIG. 13. The latitude–height distribution of the (a) zonal mean vertical p-velocity (ω) of the standard experiment and (b) the difference of zonal mean vertical velocity over the continent in February for the 15°S–15°N case. Units are in 10^{-3} mb s^{-1}.

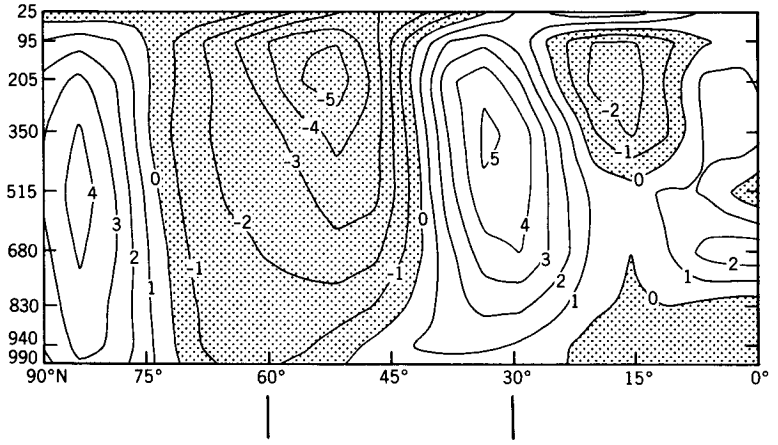

FIG. 14. The latitude–height distribution of the difference of the August zonal mean wind m s^{-1} between the perturbed 30°N–60°N and the standard experiment.

drological processes. The increase in soil moisture increases the rate of evaporation and the water vapor content of the atmosphere. This, in turn, increases the precipitation. The increase of precipitation adds more water to the ground, providing a feedback. Since some water vapor will be transported out of the region, this feedback can only last for a certain length of time. It is noted that the persistence of this feedback process depends significantly upon the latitude of an irrigated belt.

It is found that the large-scale irrigation can enhance hydrological processes not only in the region where irrigation takes place but also in adjacent regions, especially the nearby rain belts. It may also be of interest to note that the anomalous upward motion produced by irrigation may induce downward motion in a nearby area. In this area the precipitation may be reduced. The non-local impacts of a soil moisture anomaly were also noted by Manabe (1975).

The influence of large-scale irrigation is highly dependent on the climatic regime. In an arid zone where there is usually descending motion, the irrigated water will largely be used for evaporation, and comparatively little increase in precipitation would be induced. On the other hand in wet areas where there is usually ascending motion, along with the increase of evaporation, the precipitation process can be greatly enhanced. This is an unfortunate conclusion for practical agricultural purposes but not an unexpected one.

In the model subtropics from where moisture is exported to the neighboring rainbelts, a positive anomaly persists for a shorter period than a similar anomaly located in the middle latitude rainbelt where moisture tends to be recycled *in situ*. Therefore, it is surprising that this subtropical anomaly persists more than the same type of anomaly located in the tropical rainbelt of the model where moisture is more likely to be recycled. Since the temporal variability of rainfall is very large in the model tropics, a major fraction of the precipitated water is lost to runoff. This accounts for the relatively small persistence of the tropical anomaly mentioned above.

From the discussion in the previous paragraph, it is clear that the runoff plays an important role in determining the persistence of a soil moisture anomaly. As pointed out above, the fraction of precipitated water which results in runoff is large in the area where the precipitation rate undergoes a rapid temporal fluctuation. It is also expected to be larger in the region where the field capacity of the soil is small. Although it is assumed that the field capacity of soil moisture is constant everywhere in the present study, the alteration of this quantity can significantly affect the soil moisture persistence.

The change in the water balance results in changes of the thermal balance of the soil. It is found that there is a large increase of ventilation of the model surface caused by the relatively large increase of evaporation, which reduces the surface temperature especially during the first two months of the integrations. This increased latent heat from the model surface is compensated mainly by reduced heat losses of both long wave radiation and sensible heat.

The thermal state of the atmosphere is also influenced by the large-scale irrigation. In general, a sheet of cold air in the lower layer of the atmosphere is produced over the irrigated areas by increased evaporation from the wetter land surface, and a layer of warm air above the cooler region is mainly caused by the increase of latent heat release by precipitation. The change of the thermal state in the vicinity of the irrigated regions can modify the mean meridional circulation in the model atmosphere. For example, the tropical irrigation weakened the upward velocity in the tropical rainbelt. In addition, the increase or decrease of the meridional temperature gradient will re-

sult in the appropriate change of mean zonal wind speed through the thermal wind relationship.

The results from the present numerical experiments are also useful for assessing the factors that control the persistence of a soil moisture anomaly produced by natural fluctuations of climate. They indicate that, owing to recycling of moisture, a large-scale anomaly of soil moisture located in a rainbelt tends to persist longer than an anomaly located in a region of general subsidence.

In a companion paper by Yeh *et al.* (1983) we discussed the influence of snow cover removal on the persistence of a soil moisture anomaly in high latitudes. It was found that this anomaly persisted over a very long period of time because of the relatively small evaporation rate in high latitudes. This is consistent with the findings of the present study.

One of the important factors controlling the duration of a soil moisture anomaly that is not evaluated in this study is the radiation energy absorbed by the continental surface. As discussed in Section 3d, the absorbed energy essentially determines the rate of potential evaporation and controls the time constant for the disappearance of a soil moisture anomaly. Since the surface absorption of radiation energy is usually large in low latitudes, it is expected that the duration of a soil moisture anomaly tends to be shorter with decreasing latitudes. From these considerations, one can infer that, had we assumed the winter insolation for the 30°N–60°N experiment, the duration of the positive anomaly of soil moisture would have been much longer than the corresponding duration periods in the other two experiments conducted at lower latitudes. The influence of insolation upon the persistence of a soil moisture anomaly is the subject of future investigation.

One of the main deficiencies of the present study is that it was carried out under the assumption of fixed cloudiness and, therefore, clouds were not allowed to respond to changing conditions of moisture and temperature. For example, lower tropospheric moisture content increased whereas the temperature over the irrigated areas decreased. These two conditions, taken together, imply an increase of relative humidity at low levels. This, in theory, could cause more low clouds to form, reducing insolation and possibly evaporation/precipitation. However at present, it is not possible to evaluate quantitatively the effect of cloud feedback since no reliable method of cloud prediction has yet been developed. Nevertheless, a relatively simple method of cloud prediction could be incorporated into the present model to obtain a preliminary estimate of this feedback process.

It was stated in Section 2 that this particular study was performed in order to identify various physical mechanisms responsible for maintaining the soil moisture anomalies created by irrigation rather than obtaining quantitative evaluations for these processes. Future investigation of this problem could include the use of more sophisticated GCMs to obtain a more realistic description and interaction of the various processes identified in the present study.

In the current investigation, the irrigated regions or anomalies extended for the entire width of the idealized continent and persisted for a fairly long period of time. However, as the size of the anomaly is decreased, the corresponding effect that the anomaly will have on the climate may also be expected to decrease. For example, if an irrigated region is located under a rainbelt, its area must be large enough so that the enhanced precipitation will still occur over the irrigated region and contribute to the persistence of the anomaly. Therefore, it would be worthwhile to investigate how the behavior of a soil moisture anomaly depends upon the spatial scale of the anomaly.

Acknowledgments. One of the authors, T. C. Yeh, wishes to thank Dr. J. Smagorinsky for his kind invitation to visit GFDL. Through his arrangement, it was possible for this author to realize this visit. During

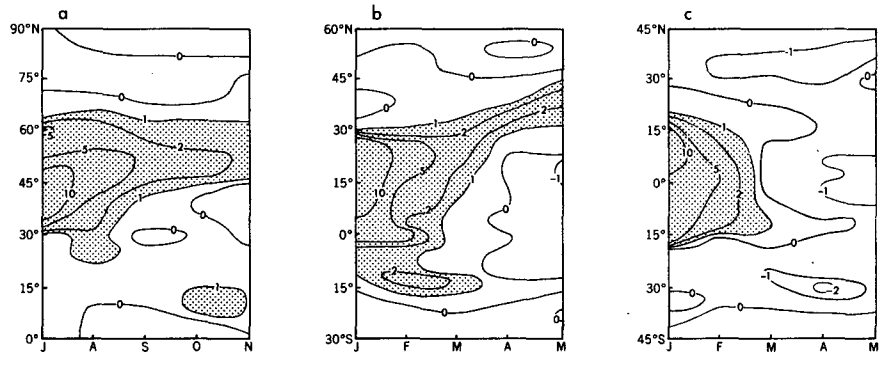

FIG. A1. Student's *t* analysis performed on the difference of zonal mean soil moisture between the perturbed and standard experiments. Values are normalized by the critical value of *t* at the 90% confidence limit for a sample size of four. Results are shown for the (a) 30°N–60°N case, (b) 0–30°N case, and (c) 15°S–15°N case.

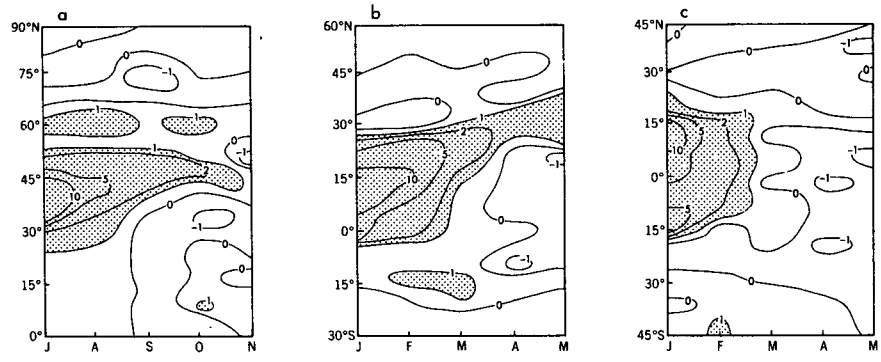

FIG. A2. Student's t analysis performed on the difference of zonal mean evaporation rate between the perturbed and standard experiments. Values are normalized by the critical value of t at the 90% confidence limit for a sample size of four. Results are shown for the: (a) 30°N–60°N case, (b) 0–30°N case, and (c) 15°S–15°N case.

the author's stay at GFDL Dr. Smagorinsky's generous hospitality was greatly appreciated. To the Geophysical Fluid Dynamics Program of Princeton University, this author wishes to express his gratitude for all the arrangements made for him. The help of the members of GFDL who in one way or another made his stay very pleasant is also greatly acknowledged. Finally this author also wishes to thank Dr. T. Malone who on behalf of the U.S. National Academy of Sciences initiated this invitation.

All three authors would like to express their appreciation to N.-C. Lau, K. Miyakoda and K. Bowman for their constructive comments on a preliminary version of the manuscript. The authors would also like to thank J. Kennedy, P. Tunison, J. Connor, M. Zadworny and W. Ellis for their prompt and efficient assistance in the preparation of the manuscript and figures.

APPENDIX

Statistical Significance

A Student's t test is performed upon the various hydrologic difference distributions shown in Section 3a, b, c for each of the three cases considered in this study. The procedure for evaluating the Student's t distribution is described in Manabe *et al.* (1981) and is applied to the present work in exactly the same way as in that previous investigation. Here, Fig. A1 represents the Student's t analysis of the soil moisture difference distributions shown in Fig. 4, Fig. A2 is the Student's t analysis of the evaporation difference distributions shown in Fig. 6, and Fig. A3 is the Student's t analysis of the precipitation difference distributions shown in Fig. 7, respectively. For all of these Student's t distributions, the t-values are normalized by the critical value of t that corresponds to the 90% confidence level for a sample size of 4 or 6 degrees of freedom. Therefore, any value shown that is greater than the absolute value of unity represents an area where the null hypothesis that the indicated difference is zero may be rejected at the 90% confidence level.

In order to determine the degree of statistical significance to the reduction of vertical motion described in Section 5b, a Student's t test was performed on the difference of zonal mean vertical velocity given in Fig. 13b. The results of this analysis are shown in Fig. A4 and indicate that the reduction of upward velocity in

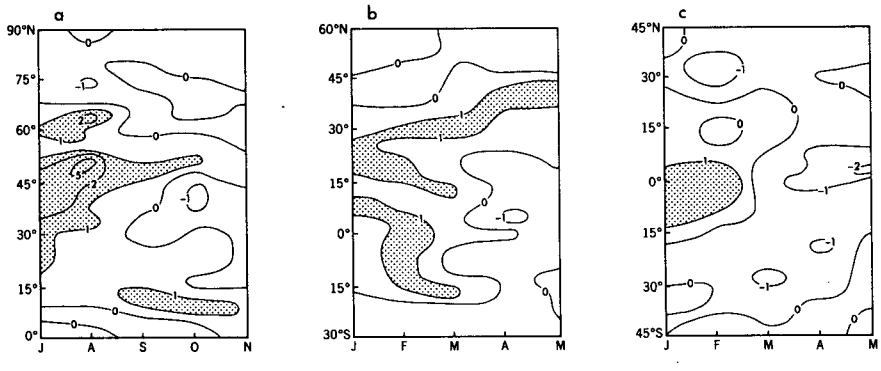

FIG. A3. Student's t analysis performed on the difference of zonal mean precipitation rate between the perturbed and standard experiments. Values are normalized by the critical value of t at the 90% confidence limit for a sample size of four. Results are shown for the: (a) 30°N–60°N case, (b) 0–30°N case, and (c) 15°S–15°N case.

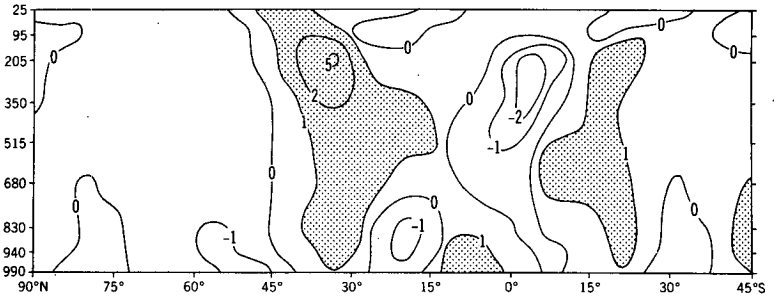

FIG. A4. Student's t analysis performed on the difference of zonal mean vertical velocity over the continent for the 15°S–15°N case. Values are normalized by the critical value of t at the 90% confidence limit for a sample size of four.

the tropical rainbelt is significant to the 90% confidence level (see shaded region centered approximately at 15°S latitude). As done previously for Figs. A1–A3, the values are normalized by the critical value of t at the 90% confidence level for a sample size of 4.

REFERENCES

Bryan, K. 1969: Climate and the ocean circulation: III. The ocean model. *Mon. Wea. Rev.*, **97**, 806–827.

Kurbatkin, G. P., S. Manabe and D. G. Hahn, 1979: The moisture content of the continents and the intensity of summer monsoon circulation.. *Meteor. Gidrol.*, **11**, 5–11.

Lacis, A. A., and J. E. Hansen, 1974: A parameterization for the absorption of solar radiation in the earth's atmosphere. *J. Atmos. Sci.*, **31**, 118–133.

Manabe, S., 1969: Climate and ocean circulation. I. The atmospheric circulation and the hydrology of the earth's surface. *Mon. Wea. Rev.*, **97**, 739–744.

——, 1975: A study of the interaction between the hydrological cycle and climate using a mathematical model of the atmosphere. Report on meeting on weather–food interactions, Massachusetts Institute of Technology, 21–45.

——, and R. J. Stouffer, 1980: Sensitivity of a global climate model to an increase of CO_2-concentration in the atmosphere. *J. Geophys. Res.*, **85**, 5529–5554.

——, J. Smagorinsky and R. F. Strickler, 1965: Simulated climatology of a general circulation model with a hydrologic cycle. *Mon. Wea. Rev.*, **93**, 769–798.

——, R. T. Wetherald and R. J. Stouffer, 1981: Summer dryness due to an increase of atmospheric CO_2 concentration. *Climate Change*, **3**, 347–386.

Namias, J. 1962: Influences of abnormal surface heat sources and sinks on atmospheric behavior. *Proc. Int. Symp. Numerical Weather Prediction*, Tokyo, 7–13 November 1960. Meteor. Soc. Japan, c/o Japan Meteor. Agency. 1-3-4, Ote-machi, Chiyoda-ku, Tokyo, Japan, 615–627.

——, 1963: Surface–atmosphere interactions as fundamental causes of drought and other climatic fluctuations. *Arid Zone Research*, Vol. 20, *Changes of Climate. Proc. of Rome Symp.* UNESCO, 75700 Paris, France, 345–359.

Rind, D., 1982: The influence of ground moisture conditions in North America on summer climate as modeled in the GISS GCM. *Mon. Wea. Rev.*, **110**, 1487–1494.

Rodgers, C. D., and C. D. Walshaw, 1966: The computation of infrared cooling rate in planetary atmospheres. *Quart. J. Roy. Meteor. Soc.*, **92**, 67–92.

Rowntree, P. R., and J. A. Bolton, 1983: Simulations of the atmospheric response to soil moisture anomalies over Europe. *Quart. J. Roy. Meteor. Soc.*, **109**, 501–526.

Shukla, J., and Y. Mintz, 1982: Influence of land-surface evapotranspiration on the earth's climate. *Science*, **215**, 1498–1500.

Stone, H. M., and S. Manabe, 1968: Comparison among various numerical models designed for computing infrared cooling. *Mon. Wea. Rev.*, **96**, 735–741.

Walker, J., and P. R. Rowntree, 1977: The effect of soil moisture on circulation and rainfall in a tropical model. *Quart. J. Roy. Meteor. Soc.*, **103**, 29–46.

Wetherald, R. T., and S. Manabe, 1981: Influence of seasonal variation upon the sensitivity of a model climate. *J. Geophys. Res.*, **86**, 1194–1204.

Yeh, T.-C., R. T. Wetherald and S. Manabe, 1983: A model study of the short-term climatic and hydrologic effects of sudden snow-cover removal. *Mon. Wea. Rev.*, **111**, 1013–1024.